

AIAA 2004–2541

On Unstable 2D Basic States in Low Pressure Turbine Flows at Moderate Reynolds Numbers

N. Abdessemed and S. J. Sherwin

Department of Aeronautics

Imperial College London,

South Kensington Campus, London, SW7 2AZ, UK

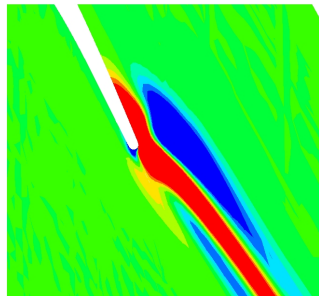
V. Theofilis

Departamento de Motopropulsion y

Termofluidodinámica,

E.T.S.I. Aeronáuticos, Universidad Politecnica de Madrid,

Pza. Cardenal Cisneros 3, E-28040 Madrid, SPAIN



34th Fluid Dynamics Conference and Exhibit
June 28 – July 1, 2004 / Portland, Oregon

On Unstable 2D Basic States in Low Pressure Turbine Flows at Moderate Reynolds Numbers

N. Abdessemed and S. J. Sherwin

Department of Aeronautics
Imperial College London,
South Kensington Campus, London, SW7 2AZ, UK

V. Theofilis

Departamento de Motopropulsion y Termo-fluidodinámica,
E.T.S.I. Aeronáuticos, Universidad Politecnica de Madrid,
Pza. Cardenal Cisneros 3, E-28040 Madrid, SPAIN

Results are presented of BiGlobal stability analysis of incompressible flow over a row of T-106/300 Low Pressure Turbine blades. In particular the two- and three-dimensional stability of a two-dimensional steady state is investigated for Reynolds numbers below 915. Both structured and unstructured meshes have been used at different degrees of refinement, while variations of the polynomial order of the numerical methods in either approach have ensured numerical convergence. The analysis shows that the transition from steady to periodic flow takes place at a Reynolds number of $Re_c = 905 \pm 10$. The flow remains linearly stable to three-dimensional disturbances below Re_c . The leading eigenvalues of the LPT flow are obtained in a range of Reynolds and spanwise wavenumber parameters. The two most interesting BiGlobal eigenmodes have been found to be related with the wake of the blade and the separated flow in the trailing-edge region on the suction side of the blade.

Nomenclature

Abbreviations

EVP	Eigenvalue problem
DNS	Direct numerical simulation
LPT	Low pressure turbine
KH/TS	Kelvin-Helmholtz/ Tollmien-Schlichting
OSE/PSE	Orr-Sommerfeld-equations/ Parabolised stability equations
c.c.	complex conjugate

Latin Symbols

Re	Reynolds number
Re_c	primary critical Reynolds number
Re_{D_c}	primary critical Reynolds number based on D
D	equivalent bluff body diameter
L_z	spanwise wavelength
$\bar{\mathbf{q}} = (\bar{u}, \bar{v}, \bar{p})^T$	steady basic flow
$\hat{\mathbf{q}} = (\hat{u}, \hat{v}, \hat{p})^T$	amplitude functions of perturbations

$\mathbf{q} = (u, v, p)^T$	transient solution
t	time
i	imaginary unit
U	velocity vector
A, B, C, D	eigenproblem matrices
p	polynomial order
h	characteristic elemental size

Greek Symbols

β	real wavenumber parameter
Ω	two-dimensional computational domain
ω	complex eigenvalue
ω_r	growth/damping rate
ω_i	circular frequency
ϵ	infinitesimal quantity
ξ	coordinate

Subscripts

i	imaginary part
r	real part

Calligraphic symbols

\mathcal{L}	$(1/Re)(\mathcal{D}_x^2 + \mathcal{D}_y^2 - \beta^2) - \bar{u}\mathcal{D}_x - \bar{v}\mathcal{D}_y$
\mathcal{D}_x	$\partial/\partial x$
\mathcal{D}_y	$\partial/\partial y$

The material is based upon work supported by the Air Force Office of Scientific Research, under Grant No. F49620-03-1-0295 to *nu-modelling S.L.*, monitored by Dr. Thomas Beutner.

Introduction

Research on control of low-pressure turbine flows has received renewed impetus recently, in line with ever increasing hardware capabilities which permit probing the range of Reynolds numbers relevant to such flows for the first time. State-of-the-art direct numerical simulation (DNS) investigations^{3,15–17} modelled the actual flow in a LPT passage, which is characterised by Reynolds numbers of order 10^5 . These investigations are based on different simplifications and modellings of the flow and the blade geometry as well as on different conceptual approaches toward the goal of flow control. Wu et.al¹⁷ performed DNS modelling the blade geometry as well as the incoming wake in order to show the connection of classic KH/TS (e.g. Kleiser and Zang⁶) and bypass transition mechanisms. It was found that instability in the chosen configuration shared principal characteristics with transient growth phenomena in archetypal flat-plate and channel flows^{4,13} Fasel *et al.*³ employed active control using two- and three-dimensional DNS in order to shed light on yet unknown instability mechanisms which may successfully improve flow performance in experiments.

Wu and Durbin¹⁶ simplified the model by neglecting the periodic wake of the stator blade and assuming the incoming flow to be parallel, which revealed the correlation between longitudinal vortices in the free stream and counter-rotating vorticity inside the boundary layer. This vorticity can be associated to algebraically growing instabilities in flat-plate boundary-layer and channel canonical flows. Both DNS studies by Durbin and co-workers have identified transient growth to be a physical effect of rather higher significance compared with mean flow deformation inside the respective boundary layer. Consequently, understanding and modelling transient growth mechanisms in this class of flows appears to be a key to devising successful flow-control methodologies; this, in turn, requires knowledge of the (BiGlobal) eigenspectrum that describes instability of LPT flows. In order to gain this basic knowledge, the present work focuses on a moderate-Reynolds number range, where the onset of primary and secondary bifurcations is expected to be.

Central to this class of investigations are the mechanisms that describe the three-dimensional nature of the instabilities of this class of flows. The computational effort that underlies three-dimensional DNS renders this numerical approach accessible only to large-scale facilities and is certainly inappropriate for parametric studies. An alternative, more efficient, methodology based on BiGlobal linear stability analysis has been chosen in the current research effort. In this context, only a two-dimensional DNS need be performed, the results of which are analysed with respect to their stability against the full range of spanwise wavenumbers at each Reynolds number.

The numerical solution of the two-dimensional

Navier-Stokes equations has been performed by means of *Nektar*, a DNS solver based on the spectral/*hp* element method.⁵ The subsequent instability analysis was also performed using a spectral element methodology, which has been shown in the past to be appropriate (as well as efficient) means to study the stability of complex flows (cf. that over a NACA0012 airfoil¹¹). The present effort is devoted to investigation of alternative spatial discretization approaches for both the DNS and the BiGlobal stability analysis, while for the latter the development of both two- and three-dimensional disturbances has been studied using the Arnoldi method, an efficient approach to calculate the most significant eigenvalues and eigenmodes of the spectrum.

Theory

Linear Stability Analysis

Central to linear flow stability research is the concept of decomposition of any flow quantity into a steady or time periodic laminar basic flow upon which small-amplitude multi-dimensional disturbances are permitted to develop. In order to transfer the idea of this basic concept to the present context, where the basic state is time-independent and homogeneous in its third dimension, we consider the two relevant decompositions, given in the following by equations (1) and (2) for the case of incompressible flow.

Transition from 2D-steady to 2D-periodic flow

Investigating the two-dimensional instability of a two-dimensional steady basic flow, the appropriate decomposition is described by

$$\mathbf{q}(x, y, t) = \bar{\mathbf{q}}(x, y) + \varepsilon \hat{\mathbf{q}}(x, y) e^{\omega t} + c.c., \quad (1)$$

where $\bar{\mathbf{q}} = (\bar{u}, \bar{v}, \bar{p})^T$ is a steady solution of the two-dimensional continuity and Navier-Stokes equations ($\bar{w} = 0$) and $\hat{\mathbf{q}} = (\hat{u}, \hat{v}, \hat{w}, \hat{p})^T$ represents the amplitude of the flow perturbation, with $\hat{w} \equiv 0$ in this case.

Transition from 2D-steady to 3D flow

In order to identify transitional states from a two- to a three-dimensional flow, the disturbance is permitted to assume a harmonic expansion in z , satisfying the Ansatz

$$\mathbf{q}(x, y, z, t) = \bar{\mathbf{q}}(x, y) + \varepsilon \hat{\mathbf{q}}(x, y) e^{[\omega t + i \beta z]} + c.c., \quad (2)$$

where the perturbation is now assumed to comprise all three velocity components and is periodic over a domain of spanwise extent $L_z = 2\pi/\beta$, where β is a real wavenumber parameter.

Eigenvalue problem

Introducing the more general equation (2) into the incompressible continuity and Navier-Stokes equations a non-linear (in terms of both $\bar{\mathbf{q}}$ and $\hat{\mathbf{q}}$) system of equations is obtained. The basic flow terms associated with

$\bar{\mathbf{q}}$ are then subtracted out and the resulting system is linearised about $\bar{\mathbf{q}}$ assuming that $\epsilon \ll 1$, to obtain the following equations

$$[\mathcal{L} - (\mathcal{D}_x \bar{u})] \hat{u} - (\mathcal{D}_y \bar{u}) \hat{v} - \mathcal{D}_x \hat{p} = \omega \hat{u}, \quad (3)$$

$$-(\mathcal{D}_x \bar{v}) \hat{u} + [\mathcal{L} - (\mathcal{D}_y \bar{v})] \hat{v} - \mathcal{D}_y \hat{p} = \omega \hat{v}, \quad (4)$$

$$\mathcal{L} \hat{w} - i \beta \hat{p} = \omega \hat{w}, \quad (5)$$

$$\mathcal{D}_x \hat{u} + \mathcal{D}_y \hat{v} + i \beta \hat{w} = 0, \quad (6)$$

which are subject to appropriate boundary conditions over the two-dimensional region Ω . For the present problem these are the no-slip condition at the surface of the turbine-blade, zero velocity at the inflow and $\partial \hat{u} / \partial n = \partial \hat{v} / \partial n = 0$ at the outflow as well as periodic connectivity of all flow quantities at the lower and upper boundaries, as illustrated in figure (1). In equations (3) - (5) we note that

$$\mathcal{L} = (1/Re)(\mathcal{D}_x^2 + \mathcal{D}_y^2 - \beta^2) \quad (7)$$

$$-\bar{u} \mathcal{D}_x - \bar{v} \mathcal{D}_y, \quad (8)$$

$$\mathcal{D}_x = \partial / \partial x \quad (9)$$

$$\mathcal{D}_y = \partial / \partial y \quad (10)$$

The system is discretised in both the x and y spatial directions, resulting in the two-dimensional, partial derivative matrix eigenvalue problem for a given set of parameters β and Re

$$A(\beta, Re) \hat{\mathbf{q}} = \omega B(\beta, Re) \hat{\mathbf{q}}. \quad (11)$$

In general the matrix-eigenvalue problem is complex and non-symmetric, although here a redefinition of \hat{w} and \hat{p} in (5-6) results in a real EVP;¹⁰ this redefinition has the advantage of halving the storage requirements for the solution of the eigenvalue problem which, in turn, is interesting since the leading dimension of the matrices A and B is proportional to the degrees of freedom used to discretise the spatial domain. Still, the large resolution requirements in combination with the relative complexity of the geometry suggest use of a spatial discretisation scheme which provides optimal accuracy at a modest resolution; the spectral/ hp element method, previously demonstrated on the problem of instability of a NACA0012 aerofoil,¹¹ has been chosen to accomplish this target.

In order to solve the time-differential form of equation (11) in an efficient manner the Arnoldi algorithm, which is based on a Krylov subspace iteration method, has been used in combination with the exponential power method. The exponential power method solves the time-differential form of equation (11)

$$\partial \mathbf{q} / \partial t = C \mathbf{q}, \quad (12)$$

which has the solution

$$\mathbf{q}(t + \Delta t) = D \mathbf{q}(t) = \mathbf{q}(t) e^{\int_t^{t+\Delta t} C d\tau}. \quad (13)$$

Employing the Arnoldi algorithm to solve equation (13) using a time-stepping scheme yields the dominant eigenvalues of $D = e^{\Delta t C}$ (where we have assumed C is independent of time) are the leading eigenvalues (i.e. the ones with the largest real part) of the matrix $\Delta t C$.¹⁴ Since only the stability-significant leading eigenvalues are calculated, the run-time associated with the total process of building the Krylov subspace and obtaining the eigenvalues of the Hessenberg matrix constructed by the iteration is a small fraction of that required by classic methods, such as the QZ algorithm.⁸

Results

Structured vs. unstructured grid generation

The spectral/ hp element method has been employed in the context of the *Nektar* code,⁵ which permits use of both structured and unstructured meshes, based on triangular and/or quadrilateral elements. In order to yield optimum performance of the computations the possibilities of the code were exploited by generating two different grids.

Figures 1 and 2 illustrate the generated meshes around a T-106/300 low-pressure turbine blade. Both meshes consist of quadrilateral elements forming a boundary layer around the blade. Outside of the boundary layer region the elements remain quadrilateral in the mesh presented in figure 1 and are triangular in the mesh presented in figure 2. Since the mesh in figure 2 consists of mainly unstructured triangular elements, it will be referred to as the *unstructured mesh*, the grid in figure 1 is referred to as the *structured mesh*.

In both cases the blade geometry is approximated by 200 coordinates, which are utilised to perform cubic b-spline interpolations to obtain a smooth blade surface representation. Results concerning convergence and accuracy using the different meshes will be given in the following sections. In order to obtain a basic understanding of the flow and its stability characteristics, initial computations were based on the less expensive structured mesh.

Identification of the critical Reynolds number for two-dimensional instability

In order to obtain the steady states as basis for the linear stability analysis, two-dimensional DNS of the flow have been performed for different Reynolds numbers in the expected range of the first two-dimensional instability. Figure 3 illustrates the vorticity of the computed domain for the flow of Reynolds numbers 890, after a steady state has been reached.

We define the Reynolds number Re as $Re = U_\infty c / \nu$, where U_∞ is the inflow velocity magnitude, c is the aerofoil chord and ν is the kinematic viscosity. Computations for $Re = 895$ lead to qualitatively analogous results, whereas the flow for $Re = 896$ becomes time-periodic as illustrated in figure 4 for a Reynolds

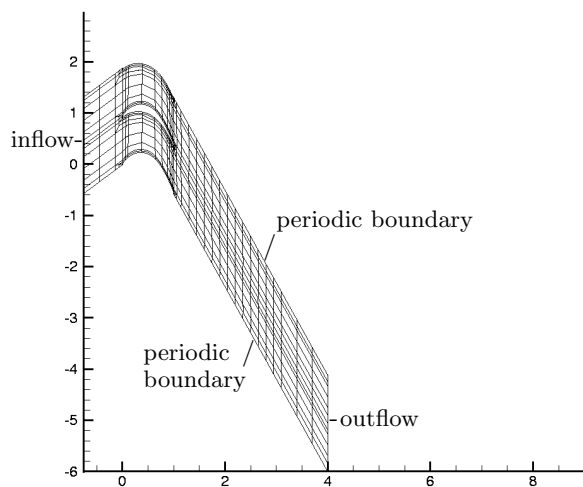


Fig. 1 Structured domain consisting of approximately 200 quadrilateral elements and collocation points using polynomial order $p=4$ (upper); detail around the LPT blade surface (lower).

number of 1000. The transition from steady state to periodic flow has hereby been identified for the mesh based on 200 structured elements. $Re = 896$ will initially be referred to as the first critical Reynolds number Re_c .

Associating this Reynolds number to an equivalent bluff body diameter D allows the comparison with the well studied flow past a circular cylinder, whose primary instability takes place at $Re_c = 46$.¹ For this purpose, the equivalent diameter D has been defined to be the distance between the local maxima of the velocities on a line as illustrated in figure 5. This line is touching the trailing edge and is perpendicular to the flow in the far wake. Describing the line using the coordinate ξ , the equivalent bluff body diameter can be expressed as

$$D = |\xi(\max_1|U|) - \xi(\max_2|U|)| \quad (14)$$

For flows close to the transitional state $D \approx 0.30c$ and hence $Re_{D_c} \approx 270$.

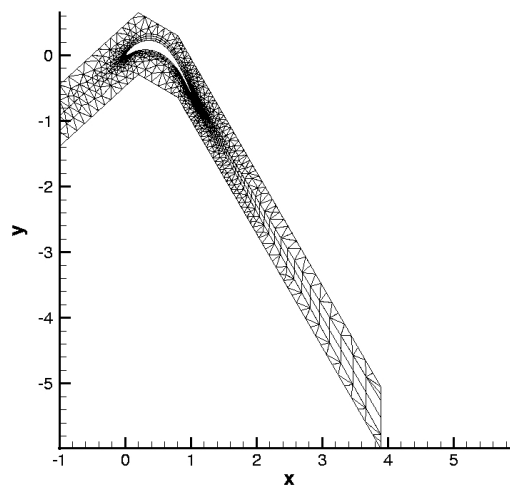


Fig. 2 Unstructured domain consisting of approximately 2000 elements (upper); detail of the trailing edge (lower).

Linear stability analysis confirms the results found by the DNS approach. Basic states at Reynolds numbers below Re_c have been analysed using the Arnoldi algorithm to compute the leading eigenvalues of the system (3-6); one result is shown in figure 6.

As the critical Reynolds number for unsteadiness is approached, increasingly long time-integration is required to reach steady state. However, a linear extrapolation of Re and the leading eigenvalue, as shown in figure 6, suggests that the flow becomes unstable to two-dimensional disturbances at $Re \approx 897$. This result is consistent (though slightly different) with that of the DNS. The least stable eigenmodes at $Re = 820$ and $Re = 893$ are shown in terms of amplitude functions of the disturbance flow vorticity in figure 7; we term this structure the *wake mode*. As the critical Reynolds number for amplification of two-dimensional disturbances is approached, the intensity of the wake mode increases and the amplitude function tends toward the trailing edge.

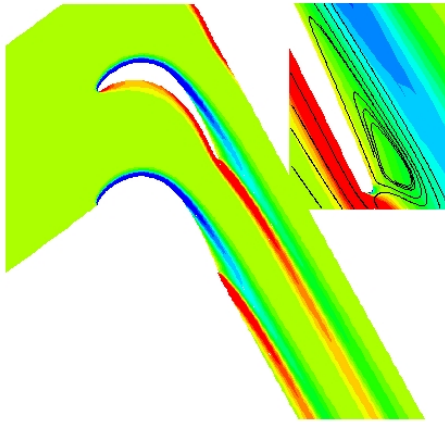


Fig. 3 Time-independent base flow vorticity for $Re = 890$ obtained using 200 structured elements and 7th-order polynomials

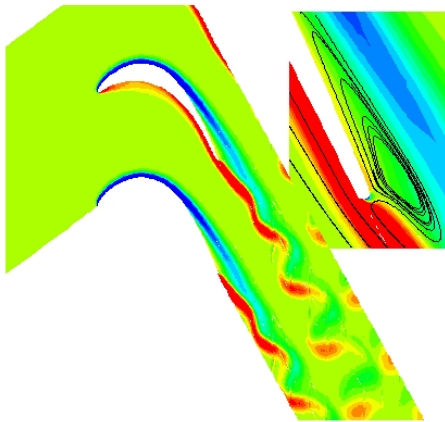


Fig. 4 Time-periodic base flow vorticity for $Re = 1000$

h-refinement

The integrity of our results is demonstrated by employing the unstructured mesh to deliver results practically identical to the above. A mesh refinement using unstructured triangular elements allows a more flexible distribution of mesh density at specific locations of interest and of necessary resolution at the trailing and leading edge. In order to ensure adequate *h*-refinement with the unstructured mesh, the number of elements was increased by up to an order of magnitude when compared to the structured grid. This necessarily results in higher computational cost per time step when using the unstructured mesh. Comparisons of the results using the structured mesh and

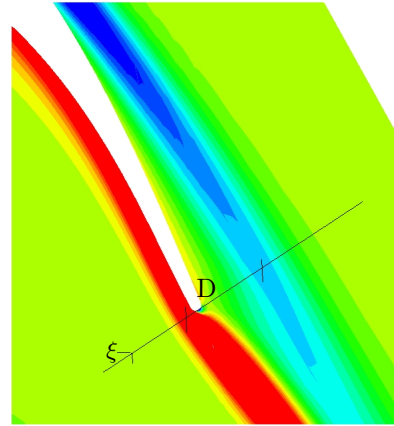


Fig. 5 Determination of the equivalent bluff body diameter D

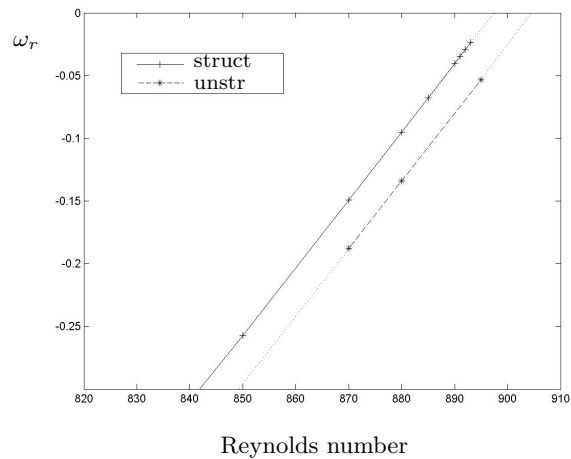


Fig. 6 Linear correlation between Reynolds number and growth rate of the leading eigenvalue, structured and unstructured mesh.

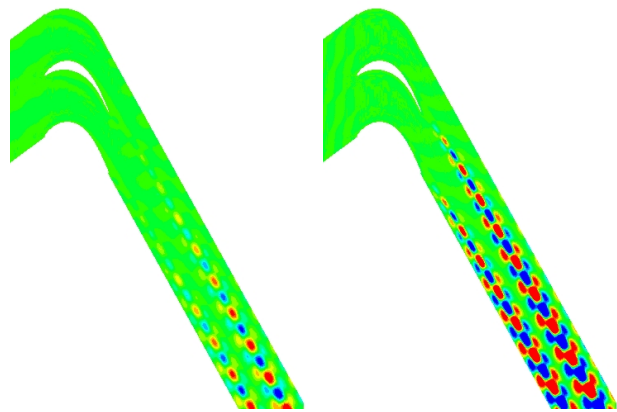


Fig. 7 Least stable eigenmode for $Re = 820$ (left) and $Re = 893$ (right, same isocontours)

element count	leading eigenvl.	damping- rate ω_r	frequency ω_i
Structured Grid (224 elements)	ω_1 ω_2	-0.557930 -1.119470	± 2.08443
Unstructured Grid (1586 elements)	ω_1 ω_2	-0.589960 -1.04967	± 1.70023
Unstructured Grid (2028 elements)	ω_1 ω_2	-0.589963 -1.05098	± 1.70362

Table 1 Variation of mesh density and its distribution for $Re=700$ and $p=7$

different unstructured meshes with various mesh densities can be seen in table 1 at a single $Re = 700$.

The differences in the results on the damping rate of the leading eigenvalues, as generated by the inexpensive structured and either of the unstructured meshes, is confined in the third significant; that between the well-resolved unstructured meshes is of $O(10^{-6})$. In the range of stable Reynolds numbers all eigenvalues are real, although as the flow comes closer to Re_c , as illustrated by the dotted line in figure 6, convergence is increasingly challenging to obtain. The highest-Reynolds number results shown in this figure have been obtained using a refined mesh with more than 2000 unstructured elements. Extrapolation of these results leads to a prediction of critical Reynolds number for amplification of two-dimensional instabilities at $Re_c \approx 905$. Considering that both growth rate and frequency change only slightly in this range of mesh resolution, we conclude that the critical Reynolds number is $Re_c = 905 \pm 10$.

***p*-refinement**

The high-order spectral/ hp scheme has been applied using different polynomial orders p in order to investigate the correlation between the accuracy of the solution and the chosen polynomial expansion. The objective here is to employ polynomial orders of sufficient degree to describe the flow physics and yet low enough for the computations to remain efficient. Table 2 summarises results based on the structured mesh for different values of p at $Re = 870$.

Comparing the leading eigenvalue with the polynomial order shows that $p = 8$ yields satisfying results to two significant figures in terms of p -resolution. A convergence study for the unstructured mesh yields the results shown in table 3. As expected the degree polynomial to reach convergence when using an unstructured mesh is *lower* than that required by the

p	ω_r	ω_i
3	-0.213743	± 1.69066
6	-0.218046	± 1.67449
7	-0.155037	± 1.59812
8	-0.149364	± 1.58672
9	-0.153072	± 1.58980
10	-0.154779	± 1.54819
11	-0.150711	± 1.55559

Table 2 Variation of the polynomial order p and the obtained eigenvalues for $Re=870$ using Arnoldi, structured mesh

p	ω_r	ω_i
3	-0.199461	± 1.63790
5	-0.187792	± 1.62469
6	-0.187688	± 1.62462
8	-0.187697	± 1.62444
9	-0.187684	± 1.62445

Table 3 Polynomial order p and the obtained eigenvalues at $Re = 870$, unstructured mesh

structured code; $p=5$ yields satisfactory convergence to three significant figures. This result raises the question (and future task of our investigations) of optimisation of p - versus h -refinement with respect to computational effort and obtained accuracy.

Investigation of the three-dimensional instability

The question whether two- or three-dimensional instability will be the first to be observed in a given flow cannot be answered in a unique manner, except in the simple cases of instability of one-dimensional shear-flow profiles.² Even in that narrow context, numerical solutions of the boundary layer stability equations⁷ are necessary in order to shed light into the different flow ranges where two- or three-dimensional instabilities will first be amplified. In the case of two-dimensional base states evidence from a handful of analysed flows is contradictory. As an example, while the steady state of the circular cylinder first becomes unstable to two-dimensional modes through a Hopf bifurcation and subsequently through three-dimensional instability of the ensuing time-periodic state,¹ the lid-driven cavity flow becomes unstable to three-dimensional disturbances prior to the onset of 2D unsteadiness.^{9,12} It is therefore necessary to investigate three-dimensional instability of the steady flow past the LPT-blade with respect to three-dimensional disturbances.

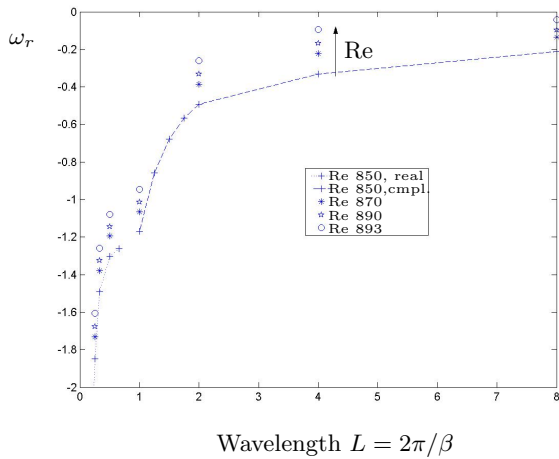


Fig. 8 Damping rates of perturbations at different wave lengths L_z . The dotted line represents the eigenvalues associated to the real eigenmodes, the dashed line the ones associated to the complex eigenmode.

Linear stability analysis has been performed based on equation (2), which introduces the decomposition of the flow into a two-dimensional base flow and a three-dimensional perturbation, seeking results by parameter studies based on changing β at a fixed Re , in a range of subcritical Reynolds numbers.

Each symbol in figure 8 represents a constant Reynolds number. All real-parts of the eigenvalues remain negative, with a tendency toward the positive complex plane for increasing Reynolds number and decreasing β , suggesting that three-dimensional linear instability does not occur below Re_c . The eigenvalues obtained for $L_z < 2/3$ are real, the ones obtained for $L_z > 1$ are complex and so are the associated eigenmodes as shown in figures 10 and 11. Interestingly, it appears that the long-(spanwise)-wavelength results shown in figure 11 are associated with the wake mode, as known from the two-dimensional analysis, while the short-wavelength results shown in figure 10 are associated with an instability arising in the trailing-edge region where separation of the basic state occurs, as seen in figure 3. We term this the *bubble-mode* instability and are currently analysing its relation to the results obtained by Fasel et al.,³ who have shown the significance of instabilities in this region in terms of control of the flow over the LPT blade surface.

Conclusions

BiGlobal stability analysis has been employed in order to investigate the eigenspectrum of a T-106/300 LPT blade under uniform incoming flow conditions. The incompressible two-dimensional laminar Navier-Stokes equations were solved using a spectral/ hp element methodology in order to obtain the steady basic state to be analyzed. This relatively straightforward numerical problem has served as testbed for different

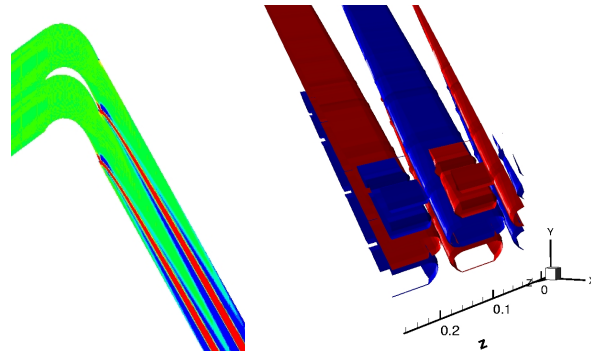


Fig. 9 Least stable eigenmode for $L_z = 0.25$ at $Re = 893$

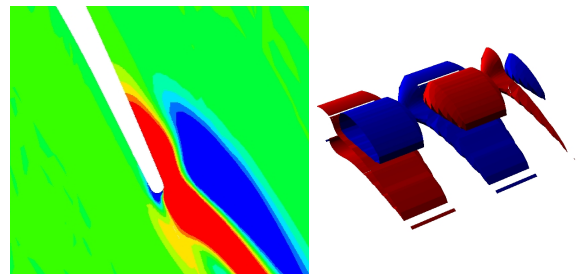


Fig. 10 Least stable eigenmode for $L_z = 0.25$ at $Re = 893$, magnification of the trailing edge

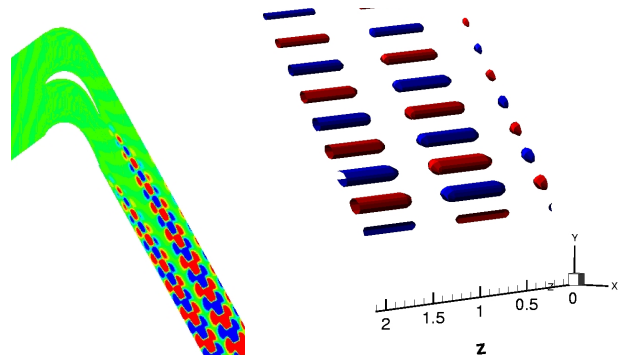


Fig. 11 Least stable eigenmode for $L_z = 2$ at $Re = 893$

meshing strategies, one based on structured and one on unstructured domain decomposition. h - as well as p - refinements have been performed with either type of grid in order to achieve convergence. An efficient algorithm for the recovery of the most interesting part of the eigenspectrum has subsequently been utilized in order to analyse the basic state with respect to both two- and three-dimensional instability.

The critical Reynolds number for two-dimensional instability has been identified in the range $Re_c = 905 \pm 10$ for the first time. Consistency between DNS and linear stability analysis supports this result. Further numerical experimentation, modifying the extent of the computational domain and introducing further

mesh-refinement, is expected to narrow the presented range of Re_c in the near future. Investigations concerning three-dimensional instability, for a range of spanwise wavenumbers below Re_c , yielded two results of significance. First, the two-dimensional flow has been shown to be the first to become unstable; second, the two least-damped eigenmodes are related with the wake of the blade and the separation region near its trailing edge.

With the present numerical experimentation concluded, the results obtained have opened several avenues for future research from a physical point of view. One interesting question, which is currently actively pursued, is that of instability of the time-periodic basic state set up at $Re > Re_c$. Answering this question requires slightly modified algorithms in order to capture the expected onset of three-dimensionality as well as the linear stability characteristics of the most significant Floquet eigenmodes. A different aspect to be pursued, once the eigenspectrum of the LPT is documented in detail, in a study of the pseudospectrum of this blade and its relation to transient growth in the LPT passage. Both questions are currently actively pursued in order to shed light onto the fundamental instability mechanisms of this technologically significant flow.

References

- ¹D. Barkley and R.D. Henderson. Three-dimensional floquet stability analysis of the wake of a circular cylinder. *J. Fluid Mech.*, 322:215 – 241, 1996.
- ²P.G. Drazin and W.H. Reid. *Hydrodynamic stability*. Cambridge University Press, 1981.
- ³H. F. Fasel, A. Gross, and D. Postl. Control of separation for low pressure turbine blades: numerical simulations. In V. Theofilis et al., editor, *Proc. of the Global Flow Instability and Control Symposium II*, Crete, Greece, June 11-13 2003, 2003.
- ⁴H. R. Grek, V. V. Kozlov, and M. P. Ramazanov. Three types of disturbances from the point source in the boundary layer. In *Proc. of the Laminar-turbulent Transition Symposium II*, pages 267–272, Novosibirsk, 1985.
- ⁵G. Em Karniadakis and S. J. Sherwin. *Spectral/hp element methods for CFD*. OUP, 1999.
- ⁶L. Kleiser and T. A. Zang. Numerical simulation of transition in wall-bounded shear flows. *Annu. Rev. Fluid Mech.*, 23:495–537, 1991.
- ⁷L. M. Mack. Boundary layer linear stability theory. In *AGARD-R-709 Special course on stability and transition of laminar flow*, pages 3.1–3.81, 1984.
- ⁸V. Theofilis. Linear instability in two spatial dimensions. In K. D. Papailiou, editor, *Fourth European Computational Fluid Dynamics Conference ECCOMAS'98*, pages 547–552, Chichester, N. York, 1998. J. Wiley and Sons.
- ⁹V. Theofilis. Globally-unstable flows in open cavities. page 12 pp. AIAA Paper 2000-1965, 2000.
- ¹⁰V. Theofilis. Advances in global linear instability of non-parallel and three-dimensional flows. *Prog. Aero. Sciences*, 39 (4):249–315, 2003.
- ¹¹V. Theofilis, D. Barkley, and S.J. Sherwin. Spectral/hp element technology for global flow instability and control. *Aero. J.*, 106:619–625, 2002.
- ¹²V. Theofilis, P. W. Duck, and J. Owen. Viscous linear stability analysis of rectangular duct and cavity flows. *J. Fluid Mech.*, 505:249–286, 2004.
- ¹³L. N. Trefethen, A. E. Trefethen, S. C. Reddy, and T. Driscoll. Hydrodynamic stability without eigenvalues. *Science*, 261:578–584, 1993.
- ¹⁴L.S. Tuckerman and D. Barkley. Bifurcation analysis for timesteppers. In E. Doedel and L.S. Tuckerman, editors, *Numerical Methods for Bifurcation Problems and Large-Scale Dynamical Systems*, volume 119, pages 543–466. Springer, New York, 2000.
- ¹⁵J.G. Wissink. Dns of separating, low reynolds number flow in a turbine cascade with incoming wakes. In W. Rodi and N. Fueyo, editors, *Proc. of the Engineering Turbulence Modelling and Experiments IV*, pages 731–740, Mallorca, Spain, 16-18 September 2002, 2002.
- ¹⁶X. Wu and P. A. Durbin. Evidence of longitudinal vortices evolved from distorted wakes in a turbine passage. *J. Fluid Mech.*, 446:199–228, 2001.
- ¹⁷X. Wu, R.G. Jacobs, J.C.R. Hunt, and P. A. Durbin. Simulation of boundary layer transition induced by periodically passing wakes. *J. Fluid Mech.*, 398:109–153, 1999.